THE SEALING SURFACE STRESS OF TUBING JOINTS HAS BEEN MODELED TO REFLECT WEAR.

M.Sathish kumar[1],Dr.B.Ravindar[2]

Assistant professor[1],Associate Professor[2]

Department Of Mechanical Engineering

Sree Chaitanya College of Engineering, Karimnagar

ABSTRACT:

As we age, tubing joints lose their tightness and integrity. Here, we examine the characteristics of the stress distribution on the sealing surface and propose a new method for determining joint wear that makes use of the numerical cutting technique. A three-dimensional model of a worn tubing junction subjected to complex stresses was created and validated using the finite element method in order to ascertain the stress distribution on the sealing surface. The failure mechanism of a worn tubing connection and the effects of interior wear on the joint were revealed by the examination of the stress distribution on the sealing surface. The results showed that the contact stress of the worn part of the sealing surface reduced as the internal wear depth increased. When the internal wear depth reaches 3.0 mm, the maximum contact stress in the worn region is 27.3% lower along the circumferential direction of the sealing surface and 35.5% lower in the axial direction compared to an unworn joint. The joint's sealing surface stress distribution is nearly equal to a new joint when the joint's outside wear is 3.0 mm or less. Because internal wear has a bigger influence on the sealing surface's stress qualities than external wear, controlling internal wear during operation is therefore more crucial than preventing external wear. The sealing belt is centered on the sealing surface and has a relatively constant width throughout two wear types and a wide variety of wear depths. By doing this, the tubing junction seal's quality is preserved.

Numerical cutting process, wear modeling, contact stress, sealing performance, and tubing joint.

I.INTRODUCTION:

Around the world, there are many wells that were ultra- deep and with ultra-high temperature and ultra-high pressure. During operation, the temperature at the bot- tom of the well can exceed 300°C; during the acid frac- turing process, bottomhole pressure can exceed more than 200 MPa. One of the major issues facing these wells was wellbore integrity failure. The frequent down- hole tool failures have caused great economic losses and brought serious safety risks. The main indicators of wellbore integrity destruction are tubular deformation and high annular pressure at the wellhead.1 In the oil and gas production, the annular pressure caused by seal failure has been a very difficult and dangerous problem to solve. Many researchers have done a lot of work in this area and achieved remarkable achievements.2–4 But they have paid more attention to the integrity of the second sealing barrier formed by packer, string and well- head device, as shown in Figure 1, and less attention to the sealing of tubing and casing joints, let alone the tightness of the worn joints.

The oil tubing string consists of a number of single tubing approximately 9 m in length connected by threaded joints. This makes the joint potentially the weakest part of the entire string. The statistics showed that 64% of tubing and casing failures occurred in joints, and as much as 86% in some oilfields.5 In recent years, the use of premium joints has significantly improved the safety of joints compared to API stan- dards joints, but in practice, most string failures were still caused by leaky seals at connections.6 In order to study the reason of

sealing failure, many scholars have used a variety of methods to analyze the mechanical properties of the sealing surface of the premium joint and have made great improvement.

Chen et al.7 and Xu et al.8 used analytical method to explore the influence of geometric features on strength and sealing performance of pipe string. However, the analytical solutions were based on some assumptions, which couldn't take into account the multiple nonlinea- rities involved in the operation of joints of pipe with complex structures.

In the studies by Wang et al.,9 Zeng et al.,10 and Jingyu and Qi,11 the experimental method was used to reflect the change of sealing performance of the joint applied with loads. However, due to the complex mesh- ing structure of pin and box, it is difficult to directly measure the strain of the sealing surface. In addition, the experimental method has the characteristics of high cost, long test cycle, and high risk. In particular, some actual complex loads are difficult to apply.

In view of the shortcomings of the above two meth- ods, numerical simulation was used more and more to carry out related studies. Among them, finite element method has been widely used. Ishimura et al.,12 Hilbert and Bergstrom,13 DeLange et al.,14 Chen et al.,15 and Chen et al.16 have done successful studies on sealing performance of joints by finite element method.
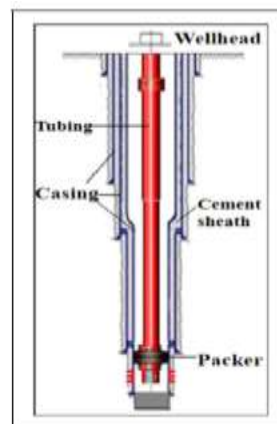

Figure 1. Well system.

What needs to be pointed out is that the current research on the mechanical characteristics of the sealing surface was mainly carried out for the unworn joint. However, under the actual working conditions, there were seriously wear at the tubing joints, and it was found that 44.7% of the wells were lost due to tubing thread during production safety inspection.17 The tub- ing is subjected to alternating loads thousands of times a day, and as the weak part of the tubing string, the integrity of joint is easy to damage due to plastic deformation caused by degradation of performance due to wear. Therefore, it is very important to pay attention to the influence of wear on its sealing performance.

In this study, a ''numerical cutting method'' was pro- posed to establish worn tubing joint model in case of internal and external wear. Then the stress characteris- tics of sealing surface were studied by the finite element method. The results could provide useful support for the research on sealing integrity of oil tubing string in ultra-deep wells.

Geometric characteristics and parameters of premium joint of tubing

17194

Ultra-deep wells that have ultra-high temperature and pressure have higher requirements on the tightness, strength, and corrosion resistance of tubing joints. Among all the premium joint products, the partial trapezoidal joint has been widely used, and its sealing per- formance can be improved by changing structural parameters. For example, the design of the auxiliary sealing surface of torque shoulder can improve the seal- ing performance, enhance the anti-compressive strength of the joint.18 Figure 2 shows the structural diagram of a typical premium joint used in the TLM oilfield, China. Its main sealing structure is metal-metal sealing mode, including three structural forms of cylinder-cylinder, cylinder-sphere and sphere-sphere, which can ensure the maximum contact pressure of the joint remains unchanged under tensile condition. At the same time, a negative 15° reverse torque shoulder was designed to make the connection have better sealing performance, as well as anti-compression and anti- over-torque performance.19–21

A three 1/2\$ tubing joint with above structure was analyzed to show the influence of internal wear on the
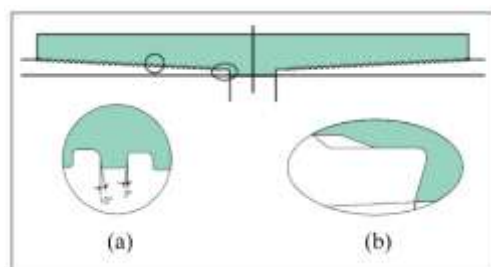
Table 1. Main geometric parameters of premium joint of oil tubing.

Parameter	Value and type
Thread profile	Trapezoid tooth
Pitch	1/6" (4.23 mm)
Thread taper	1:16
Sealing structure	The ball to the cone
	Cone taper of 1:10
	Reverse shoulder −20°
	Shoulder clearance 1.00 mm
Outer diameter of coupling	114.30 mm
Inner diameter of tubing body	76.00 mm
Outer diameter of tubing body	88.90 mm

sealing performance of the premium joint. The outer diameter R0, the inner diameter R, and the outer dia- meter of coupling R# are 88.9, 76.0, and 114.3 mm respectively. The detailed thread parameters and corre- sponding crew thread parameters are shown in Table 1.

Finite element model of tubing joint

This study selected ABAQUS to analyze the three- dimensional mechanical properties of the sealing sur- face of the tubing premium joint. In the process of solu- tion, a new stiffness matrix appears in each increment step. This makes the implicit algorithm more compli- cated than the explicit one because it requires a lot of matrix inversion calculations, which lead the explicit algorithm be selected for calculation.

Three-dimensional finite element model for tubing premium joint

Figure 3 lists the three-dimensional geometric model for three 1/2\$ tubing premium joint. The eight-node hexahedral element was selected to mesh the model. The number of element and node in the finite element model of premium joint for an unworn tubing were 280,824 and 344,277 respectively. The loads were

Figure 2. Structure of a typical kind of premium joint used in TLM oilfield: (a) thread tooth structure and (b) sealing structure.
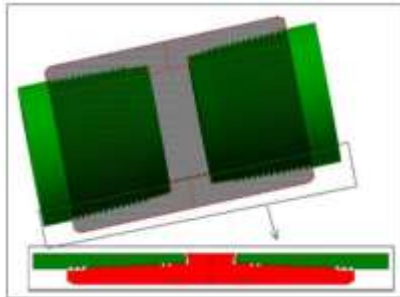
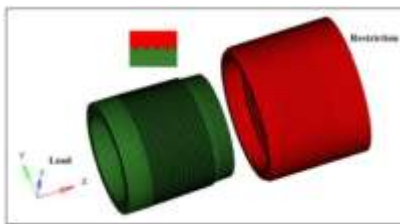Figure 3. Geometric model of premium joint of tubing.

Figure 4. Meshing and boundary conditions of tubing joint.

applied by establishing the coupling form of distribut- ing nodes on the end face of the pin, and the constraint was imposed by establishing the coupling form of kine- matical node at the end face of the box (as shown in Figure 4).

Three-dimensional finite element model for the worn tubing premium joint based on ''numerical cutting method''

In engineering practice, the failure of tubing connection is a problem that has not been solved for a long time. One of the reasons is that the study of the three- dimensional mechanical characteristics is rare for the sealing surface of worn joint of tubing. According to the field experience, there are two main forms of tubing wear: external wear and internal wear. External wear mainly appears in the outer wall of the tubing, caused by friction between the outer wall of the tubing and the inner wall of the casing, while internal wear mainly appears in the inner

wall of the tubing, caused by fric- tion between the sucker rod and the inner wall of the tubing.
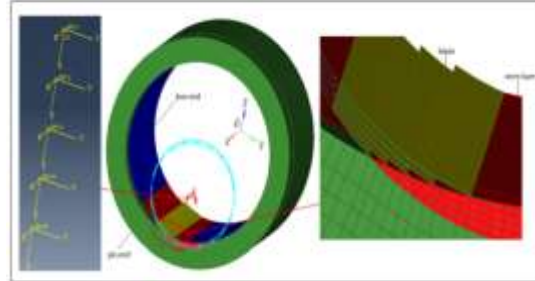

Figure 5. Establishment of an internal worn model of tubing premium joint.

Table 2. Analysis step settings.

|	Step time (s)	Load condition	
Step 1	0.00–0.20	Make-up torque	2.50 kN/m
Step 2	0.20–0.25	Axial tension	66.20 kN
Step 3	0.25–0.30	Bending moment	1.75 kN/m
Step 4	0.30–0.35	Wear	0.6 mm
	0.35–0.40	Wear	0.6 mm
	0.40–0.45	Wear	0.6 mm
	0.45–0.50	Wear	0.6 mm
	0.50–0.55	Wear	0.6 mm

The current research on the construction of worn joint model usually uses the method of wear first, then load. However, in actual working conditions, there is a causal relationship between load and wear, and the first wear may affect the calculation result because it has changed the structure of the joint already. Therefore, in this article, the numerical cutting method is used to building the wear joint model, which is more close to the actual situation of the joint.

Establishment of worn joint model. In order to establish a worn tubing modeling, a ''numerical cutting method'' was proposed based on an unworn tubing modeling. As shown in Figure 5, a worn premium joint model of tubing is listed. The red part in the figure is the wear layer, which consists of five layers of grid, and the max- imum wear depth of each layer is 0.6 mm. Five ''cut blades'' were set up, as shown in yellow part. One ''cut blade'' represents a part

17196

of the drill pipe contour and corresponds to a wear layer, and the blades and the corresponding wear layer grid are on the same circum- ference. The cut blade was set as a shell element and was made of rigid body material, its deformation was not considered during the analysis. The material para- meters of the joint were the same as those of the premium joint model of tubing, and the elasto- plasticity of the material was considered. Firstly, the unworn model was established and loaded with make-up torque, axial tension force and bending moment, and then the inner wall of the tubing was worn separately. In other words, the wear process taken place while the tubing was loaded. This approach is more in line with the actual situation of the oilfield. As shown in Table 2, four analysis steps were set up. The make-up torque was first applied in the positive x direction of the global coordinate, then the axial ten- sion was applied in the negative x direction and then the bending moment was applied in the positive y direc- tion (see Figure 5). In the actual wellbore, the outer wall of the sucker rod and the inner wall of the tubing wear out. In view of the size of the shoulder of the threaded tubing joint, when the wear depth is 4.0 mm, the deformation of the shoulder of the box is too large, so the maximum wear depth of the internal wear of the threaded tubing joint is set to 3.0 mm. Therefore, in the final analysis step, the ''blade'' was set to cut the sur- face of the tubing connection at a depth of 0.6 mm every 0.05 s to simulate the dynamic wear process. A total of five ''blades'' were set up corresponding to five wear depths, and the blades were rotated along the set paths, cutting layer by layer. The total cutting time is 0.25 s and the total wear depth is 3.0 mm.

The rotation of the blade in the fourth step was not about the global coordinate system. Instead, a local coordinate system was established along the position where the wear took place, and the blade was rotated along the x-axis direction of the newly established local cylindrical coordinate system to complete the cutting process.

Contact settings. The contact setting for tubing joint wear consisted of two parts. The first part was the face- face contact algorithm, which included three contact
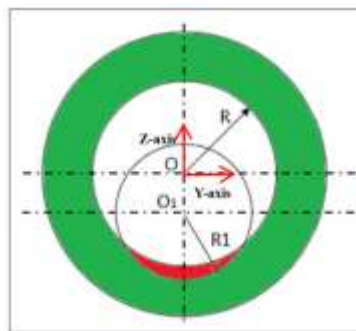
groups of pin thread tooth to box thread tooth, pin thread sealing surface to box thread sealing surface, and pin shoulder to box shoulder. The face-face contact pair algorithm should clearly indicate the contact sur- face and the subordinate relationship. The second part was to define the contact between the blade and the wear area of joint by using general contact algorithm.

In the process of building worn tubing joint model by cutting method, the setting of contact attribute should consider the contact relationship between blade and joint.

In the tangent direction, the friction property between the blade (set as rigid body) and the joint was defined as ''rough'' contact. When the blade contacted the wear layer of the joint and moved along the tangen- tial direction, the worn layer would be cut off. In the normal direction,

17197

the contact property between the blade and the joint was defined as ''hard'' contact. In view of the constant change of contact state in the cutting process, the corresponding control statements were added in the model file, so that the cutting separation surface could be extracted in real time and new contact pairs could be formed in the cutting process, so as to avoid contact state mutation caused by cutting separation as much as possible.

Criteria for chip separation. As the blade moves, chips cut from the wear layer will be separated from the joint body. There are roughly two criteria for judging whether chips are separated from the workpiece, namely, geometric criteria22 and physical criteria.23

The geometric criterion is mainly based on the change of the distance between the tool tip and the nearest node in front of the tool tip on the preprocess path to judge whether the separation is finished. When using geometric criteria, the chip is separated from the joint body by a separation line, which is the preprocess path previously mentioned. The physical criterion is defined based on the physical quantity of the element node before the tool tip, such as strain, stress and strain energy. In finite element calculation, it is considered that element node separation occurs when the corre- sponding physical quantity of element exceeds the critical value of given material. Different physical quantities will lead to form different separation criteria. Compared with geometric criteria, physical criteria has more specific physical meanings.23 Therefore, the plas- tic strain value of the element was taken as the criterion in this study, that is, the critical plastic strain value of the grid element failure was defined in the material properties. For the material used in this

model, the strain value ''shear failure'' at the time of failure is set to 0.146. When this critical value was reached, the chip was considered to separate from the joint body.

The stress characteristics on the sealing surface of tubing premium joint

Internal wear

The internal crescent wear caused by sucker rod was analyzed, as shown in Figure 6. The outer diameter of sucker rod is R1 and the inner diameter of tubing threaded joint is R.

Axial contact stress on the sealing surface. In the elastic range, good sealing performance can be guaranteed only when the contact stress is high and the contact band width is large. We selected a row of nodes along the axial direction on the sealing surface of the wear side of the pin end of tubing joint, as shown in the red nodes in Figure 7, and named it A-P (Axial Path), then observed the change of contact stress on A-P at differ- ent wear depths.

Figure 8 shows the change of contact stress along the sealing path on the side where sealing surface internal wear occurs with the different wear depths. In the model of this study, the sealing width does not change with wear depth (all is 2.87 mm), so we only focus on the change of contact stress.

As can be seen from the figure, with the increase of wear depth, the maximum contact stress along the axial path A-P is 403.4 MPa when the joint is unworn, and drops to 260.1 MPa when the joint is worn by 3 mm, decreasing by 35.5%. This is because as the wear depth increases, the stiffness of the sealing face decreases, and its bearing force decreases relative to other positions of the sealing face, so the contact stress in the wear area is relatively small. It can be found that the axial contact stress on the wear

side of the sealing surface decreases greatly when the internal wear depth increases from 0
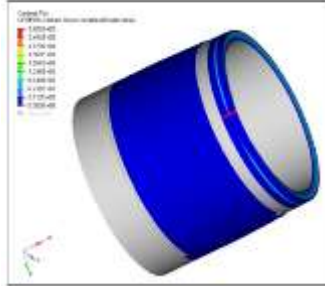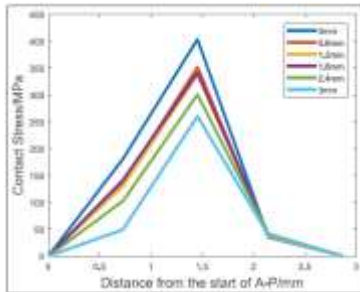

Figure 7. A-P of internal wear.

Figure 8. Contact stress on A-P at different wear depths.

to 3 mm, indicating that the internal wear seriously weakens the sealing performance of the tubing joint.

Circumferential contact stress on the sealing surface. In order to observe the change of circumferential contact stress of tubing joint when internal wear occurs, a circle of main stress points along the circumferential direction of sealing surface were selected as the circumferential path, named as C-P. See the red dots in Figure 9.

The contact stress distribution along the circumfer- ential direction of sealing surface of the internal wear joint was shown in Figure 10. It can be seen that the contact stress along the C-P of unworn joint distributes between 200 and 500 MPa, and the uneven distribution
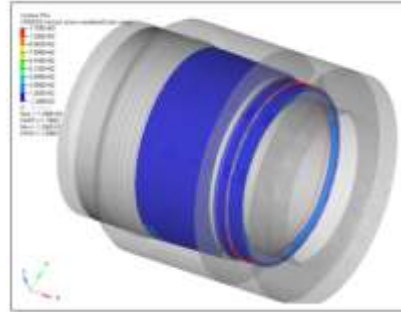

Figure 9. Circumferential path-C-P.

is caused by the friction action by make-up and the three-dimensional spiral angle existed in the screw threads. With the increase of wear depth, the stress changes significantly in the section of the wear area (as shown in Figure 10, the red dotted line circle), while there is no significant difference in stress in most areas of the circumferential circle.

As can be seen from Figure 10, the contact stress curves on the six C-Ps are closely fitted in most areas with little change under different wear quantities. Only the wear area circled by the red dotted line in the figure shows that the stress value changes greatly with wear, and the contact stress values become smaller with the increase of wear depth. It should be noted that the con- tact stress on the wear area is not the minimum one on C-P, which is due to the bending moment applied to the joint. As shown by the arrow direction in Figures 6 and 10, the bending moment is applied along the Y-axis which results in compression on the side pointed by the arrow and the contact stress in this side is relatively small. While, the contact stress on the opposite side is relatively large, and due to the action of additional ten- sion, the contact stress curve on this side has the phe- nomenon of ''flattening,'' and fluctuates less than other areas.

17199

In order to further quantify the decrease of circum-ferential contact stress with wear depth, the average con- tact stress of the wear section of sealing surface along the path of C-P were calculated, as listed in Table 3.

As can be seen from Table 3, the contact stress on the worn section of the sealing surface decreases with the increased wear depth. When the wear reaches 3 mm, the contact stress decreases from 396.3 MPa of the unworn joint to 302.3 MPa, a decrease of 27.3%. As the C-P circle point is the maximum force point along circumferential direction, this indicates that the maxi- mum stress value along the sealing direction decreases
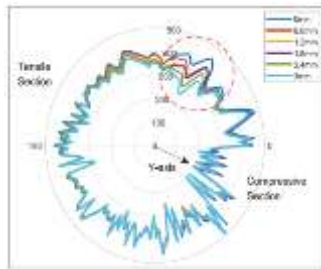

Figure 10. Contact stress on C-P at different wear depths.

Table 3. The average contact stress on C-P internal wear section.

Wear depth (mm)	0	0.6	1.2	1.8	2.4	3
Average contact stress (MPa)	396.3	364.4	351.6	353.6	325.4	302.3

seriously with an increased wear depth, which further proves that the wear will damage the sealing perfor- mance of the tubing joint.

External wear

External wear of premium joint of tubing is showed in Figure 11, that is, contact wear occurs between the outer wall (outer diameter R$) and the inner wall of the casing (inner diameter R2$). The total outer wall wear depth of the

tubing joint was also set at 3.0 mm (red part of Figure 11). Similarly, a complete tubing joint was established and applied with complex loads, then cut layer by layer.

Axial contact stress on the sealing surface. Firstly, the con- tact stress on A-P (Figure 12) on the sealing surface of the externally worn tubing joint was observed, as shown in Figure 13. The contact stress on corresponding points on A-P decreases continuously with the deepen- ing of wear, but the decreased value is very small com- pared with internal wear. When the wear reaches 3 mm, the maximum contact stress on A-P decreases from 384.5 to 369.1 MPa, which is only 4% lower than that of unworn condition. It can be seen that the external wear has little effect on the axial stress distribution of
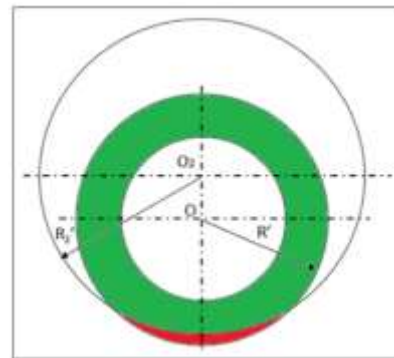

Figure 11. External wear.

the sealing surface of the tubing joint and almost no effect on the sealing performance of the joint. Circumferential contact stress on the sealing surface. The contact stress on the sealing surface of the externally worn tubing joint along the path C-P is showed in Figure 14. It can be seen that the overall contact stress distribution characteristic along circumferential circle on the sealing surface of the outer wear joint is roughly similar to that of the internal wear joint, and the distri- bution curve is also characterized by fluctuations. The contact stress curves of

17200

different wear depths fit closely and have similar form.

Table 4 shows the average contact stress of circum- ferential wear section on the sealing surface of external wear joint. It is found that with the increased wear depth, the average contact stress decreases slowly, from 375.3 MPa of the unworn joint to 348.3 MPa of 3 mm wear, only decreasing by 7.2%.

This means that the effect of external wear on the stress distribution on the sealing surface of the tubing joint is much less than that of internal wear.

Comparison and discussion

Xu et al.8 established the radial interference contact stress theoretical model of the main sealing surface of special thread joint by using the thick-walled cylinder theory of elasticity and Hertz contact mechanics theory. This model uses the section through the thread axis to cut the thread and expand it along the thread circum- ference, simplifying the ball-cone seal structure into a two-dimensional contact problem between a cylinder and a plane, as shown in Figure 15. The tangential fric- tion force is ignored, and only the normal contact stress
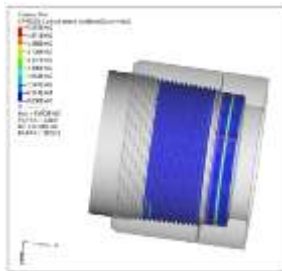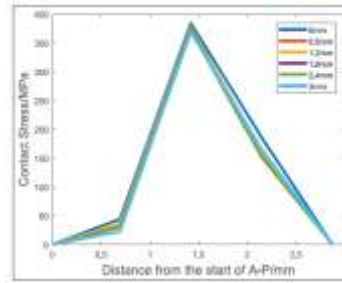

Figure 12. A-P of external wear.

Figure 13. Contact stress on A-P at different wear depths.

PsN is considered, and the following assumptions are made: (1) the contact surfaces are continuous and dis- cordant; (2) small strain; (3) tubing and contact seal structures are both regarded as elastic half-space bod- ies; (4) ignore contact surface friction.

The normal contact stress of the ball-cone sealing surface is thus obtained:

$$P_{sN}(x) = \frac{E_b E_c \sqrt{2R_s \delta_{sN} - \delta_{sN}^2 - 4x^2}}{4R_s \left[E_c \left(1 - \nu_p^2 \right) + E_b \left(1 - \nu_c^2 \right) \right]} \quad (1)$$

Where, PsN(x) is the normal contact stress at position x, MPa; Eb and Ec are respectively the elastic modulus
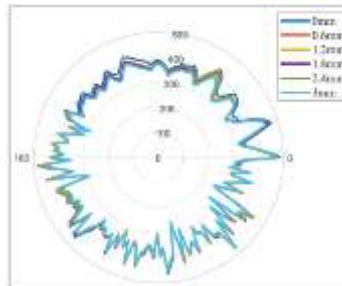

Figure 14. Contact stress on C-P at different wear depths.

of the tube body and the joint, MPa; Rs is the radius of the sphere, mm; dsN is the normal interference of the spherical surface and the cone at the initial contact point after the N turn of the make-up, mm; the np and nc are the Poisson

17201

ratios of the tube body and the joint, respectively, and are dimensionless. dsN can be determined by the following formula:

$$\delta_{sN} = N_s P \sin \gamma_S \qquad (2)$$

Where Ns is the number of make-up loops attached to the sealing surface, loops; P is pitch, mm; gs is the sealing surface half cone angle, degree.

For the model in this article, it is a special threaded tubing joint of P110 steel grade with an OD of

114.3 mm and a wall thickness of 6.45 mm, the elastic modulus of the tube body and joint are both Eb = Ec = 210,000 MPa, the Poisson ratio of the tube body and joint are vp = vc = 0.29, and the radius of the sphere is 15.0 mm. By plugging these parameters into equation (1), we can obtain

$$P_{sN}(x) = 1910.689 \sqrt{30\delta_{sN} - \delta_{sN}^2 - 4x^2} \qquad (3)$$

The make-up torque is 2.5 kN/m, which is converted to 0.05 turns. Substituting Ns=0.05, taper 1:16 and pitch 4.23mm into equation (2), the corresponding interference of sealing surface at this time can be obtained dsN =0.006mm. Substituting the interference into equation (3), the contact stress distribution calculated by analytical method can be obtained as follows:

$$P_{sN}(x) = 1910.689 \sqrt{0.18 - 4x^2} \qquad (4)$$

Figure 16 is a comparison between the contact stress curve calculated by the formula (4) and the contact
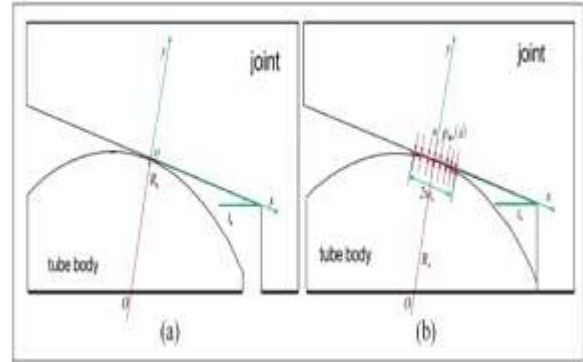

Figure 15. Schematic diagram of ball sealing facing cone: (a) initial contact and (b) final contact.
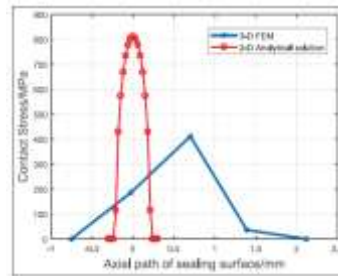

Figure 16. Comparison diagram of contact stress of sealing surface under make-up torque calculated by analytical method and finite element method.

stress translated by coordinates on the A-P path of the unworn model by finite element method in this article.

As can be seen from Figure 16, the axial distribution of contact stress obtained by two-dimensional analytical method presents a regular semi-elliptic shape, in which the initial contact area stress is high and gradually decreases along the edges of both ends, with a maximum value of 810.6 MPa, and the width of the sealing contact belt is 0.49 mm. The contact stress simulated by the three- dimensional finite element method is approximately para- bolic in axial direction, forming a sealing belt with higher contact stress and wider sealing belt on

Table 4. The average contact stress on C-P external wear section.

Wear depth (mm)	0	0.6	1.2	1.8	2.4	3
Average contact stress (MPa)	375.3	362.6	361.5	357.8	353.6	348.1

17202

the whole, which is quite different from the contact stress characteristics of the sealing surface calculated by the analytical method. The maximum contact stress value is 411.3 MPa. The bandwidth of the sealing surface is 2.87 mm. The reason for such a big difference in results is the analytical method uses linear elastic materials, the stress value will increase linearly, resulting in a larger maximum stress value. Moreover, since it is a two-dimensional model, the three-dimensional lifting Angle is not considered. However, the finite element method uses elastic-plastic materials and considers the spiral Angle, so the results are more in line with the actual situation, this also shows the necessity of three-dimensional model and nonlinear calculation.

Conclusion

In this paper, we introduced the "numerical cutting method" for modeling the worn tubing joint. This approach is more accurate than the traditional construction method and allows for the effective implementation of a three-dimensional finite element nonlinear computation in the model. The mechanical properties of the tubing joint seal surface with internal and external wear were disclosed by the finite element computation. The following conclusions can be made:

(1) Under complex loads, the "numerical cutting method" as suggested in this study can be utilized to build a worn premium joint in oil tubing. In the future, this technique can also be applied to model dynamic wear processes.

Within the parameters of this study's calculations, the impact of external wear on the sealing surface's stress distribution is negligible. When a sealing surface is subjected to external wear, its stress distribution resembles that of an unworn joint.

(3) A higher contact pressure and a wider sealing belt are the primary determinants of the premium joint's metal-metal sealing surface's sealing effectiveness. Internal wear clearly lowers the local contact stress of the sealing surface at the wear component, making it more likely that a leakage channel will emerge and sealing failure will occur. Preventing internal wear during operation should receive more attention.

Declaration of conflicting interests

The author(s) declared no potential conflicts of interest with respect to the research, authorship, and/or publication of this article.

Funding

References

1. Jun L, Shidong D, Lihong H, et al. Research progress on failure mechanism and control method of shale gas mul- tistage fracturing wellbore integrity. Petroleum Pipe Instrum 2020; 6: 10–15.

2. Buchmiler DR, Rengard O and Haug LT. Advancements in structural well integrity design and operation. In: Off- shore technology conference, Houston, TX, USA, 2012.

3. Honglin XU. Study on joint strength and sealing theory for casing and tubing premium connections. Chengdu: Southwest Petroleum University, 2015.

4. Khodami E, Ramezanzadeh A and Noroozi M. Numeri- cal modeling of oil well

integrity with a particular view to cement (case study: Maroon oilfield in southwest of Iran). J Pet Sci Eng 2021; 196: 107991.

5. Xiaowen C and Gao L. Development status of special joint of oil casing in China. Welded Pipe 2008; 4: 41–44 + 94.

6. Han XIN. Study on sealing characteristics and sealing cri- terion of special threaded joint under dynamic load. Xi'an: Xi'an University of Petroleum, 2020.

7. Chen Z, Zhu W, Di Q, et al. Prediction of burst pressure of pipes with geometric eccentricity. J Press Vessel Tech- nol 2015; 137: 1–8.

8. Xu H, Li T, Yang B, et al. Theoretical analysis of sphere to cone sealing performance for tubing and casing pre- mium connection. J Southwest Petroleum Univ 2016; 38: 179–184.

9. Wang X, Xia B and Wang Q. Experimental research on temperature field distribution of API 10-round thread connection during makeup and breakout process. Geos- ciences 2004; 18: 591–594.

10. Zeng XK, Su HH and Wang CS. Experimental research on seal ring in the pipeline mixed with r-EPDM. Adv Polym Sci Eng 2011; 221: 490–494.

11. Jingyu M and Qi A. Simulating experiment on sealing performance of shouldered face for tubing and casing connection. J East China Univ Sci Technol 2017; 43: 443–448.

12. Ishimura M, Katsuo M, Sawa T, et al. Finite element stress analysis and evaluation of the sealing performance in pipe fittings with adhesive for threaded connections under internal pressure and bending moment. In: ASME 2005 international mechanical engineering congress and exposition (ASMEDC), Orlando, FL: ASMEDC, 2005, vol. 118, pp.795–801.

13. Hilbert LB and Bergstrom J. Evaluating pressure integ- rity of polymer ring seals for threaded connections in HP/HT wells and expandable casing. SPE J 2008; 13: 123–132.

14. DeLange R, Gandikota R and Osburn S. A major advancement in expandable connection performance, enabling reliable gastight expandable connections. SPE Drill Complet 2011; 26: 412–418.

15. Chen F, Di Q, Li N, et al. Determination of operating load limits for rotary shouldered connections with three- dimensional finite element analysis. J Pet Sci Eng 2015; 133: 622–632.

16. Chen W, Di Q, Zhang H, et al. The sealing mechanism of tubing and casing premium threaded connections under complex loads. J Pet Sci Eng 2018; 171: 724–730.

17. Wei Y. Cause analysis and countermeasures of oil well tubing thread leakage. Neijiang Sci Technol 2011; 2: 53.

18. Pan X. Research on integrity of casing special threaded joint. Chengdu: Southwest Petroleum University, 2019.

19. Weijun D and Zhonghua Z. Development of steel tube product technology in Baosteel. Steel Tube 2014; 43: 9–16.

20. Fu Y, Guoquan Q, Wei Z, et al. Design and domestic product status of special thread oil casing. Petroleum Field Mach 2012; 41: 72–76.

21. Bao Iron and Steel Co., Ltd. Oil well pipe manual. Shanghai: Baoshan Iron and Steel Co., Ltd, 2018.

22. Fu J. Physical simulation and experimental study on machining process of difficult-to-machined metal materials. Changsha: Hunan University, 2013.

17204

23.   Guo J. Research on dynamics of metal cutting process based on different tool-chip friction models. Taiyuan: Taiyuan University of Technology, 2010.